





polarization plane of the exciting light acquires over a thickness  $d$  an ellipticity

$$\xi = \frac{\omega_0}{2\omega_0} \operatorname{Re} [\psi_2(\operatorname{res}(\mathbf{k}_1, \omega; \mathbf{e}_1, \omega_0) - \psi_2(\operatorname{res}(\mathbf{k}_1, \omega; \mathbf{e}_1, \omega_0))] = \frac{2}{3} \Theta(\omega, \omega_0), \quad (17)$$

where  $\Theta(\omega, \omega_0)$  is defined by Eq. (12).

If the difference  $(\omega_1 - \omega)$  is comparable in magnitude with the hole damping, Eq. (12) for the rotation angle is not valid, and to solve the problem we have to determine the hole density matrix with allowance for the blurring of the hole energy states. Here, we shall consider the case of almost parallel beams, with

$$\frac{\hbar k_2}{m_1} |\mathbf{q} - \mathbf{q}_0| \ll \tau_{12}, \quad (18)$$

recall that  $k_0 = (2\pi\omega_0/\hbar)^{1/2}$ . Moreover, we neglect as before the light wave number in comparison with the hole wave number  $k_0$ , and take no account of the contribution to  $\Delta\psi(\operatorname{res})$  from holes that have had one or more collisions. The hole density matrix components

$$\rho_{11} = \rho_{22, m_1, 1, 2m}(\mathbf{k}, 0), \quad \rho_{21} = \rho_{22, m_1, 2m}(\mathbf{k}, 0), \quad \text{and} \quad \rho_{12} = \rho_{21, m_1, 1, 2m}(\mathbf{k}, 0)$$

then satisfy the equations

$$\begin{aligned} \dot{\rho}_{11} + i(\omega_{1k} - \omega_{10}) + \tau_{1k} + \tau_{12} \dot{\rho}_{11} &= -\frac{e}{2m_0c} (\mu_1 - \mu_2) [\rho_{21, m_1, 1, 2m}(\mathbf{k}) \\ &\times \langle \delta\psi_1^{(1)} e^{i\omega t} + \delta\psi_1^{(2)} e^{-i\omega t} \rangle], \\ \dot{\rho}_{12} + 2\tau_{12} \rho_{12} &= (-i)^2 \frac{2\pi}{\hbar m_0c} \operatorname{Re} [\langle \rho_{21, m_1, 1, 2m}(\mathbf{k}) \langle \delta\psi_1^{(1)} e^{i\omega t} + \delta\psi_1^{(2)} e^{-i\omega t} \rangle \rangle_{\text{fr}}], \end{aligned} \quad (19)$$

where  $\delta\psi_1$  and  $\delta\psi_2$  are the complex vector amplitudes of the electric fields of the weak and strong light waves, and because the frequencies  $\omega$  and  $\omega_0$  are close together the difference between them has been neglected except in the time exponents. System (19) is equivalent<sup>6</sup> to the corresponding equations for a two-level quantum system with transition frequency  $(\omega_{1k} - \omega_{10})$  and damping constants  $\gamma_{1k}$  and  $\gamma_{12}$ , for which spontaneous transitions  $2 \rightarrow 1$  may be neglected. The analogy between optical transitions of holes between subbands 2 and 1 and those in two-level quantum systems has already been noted<sup>1,2</sup> in a study of the p-type germanium absorption coefficient decrease under strong illumination. The change in the permittivity tensor in the resonance approximation, used in the present study, is given by

$$\begin{aligned} \ln(\mathbf{e}_1, \omega; \psi_1(\omega_0, \omega_0) | \mathcal{E}) \\ = \frac{i\omega}{m_0c} \sum_{\mathbf{k}_1, \omega_1 = \pm \omega_0} (\mathbf{P}_{21, m_1, 1, 2m}(\mathbf{k}))^* \rho_{21, m_1, 1, 2m}(\mathbf{k}, \omega_0) \end{aligned} \quad (20)$$

where  $\rho_{21}(\mathbf{k}, \omega)$  is the density matrix amplitude at frequency  $\omega$ .

With system (19), we can find  $\rho_{21, m_1, 1, 2m}(\mathbf{k}, \omega)$  in the second order relative to the strong field amplitude and the first order relative to the probe field amplitude. After substituting in Eq. (20) the expression found for  $\rho_{21, m_1, 1, 2m}(\mathbf{k}, \omega)$ , summing over  $m$ , and integrating over  $\mathbf{k}$ , we finally obtain for the specific rotation angle

$$\begin{aligned} \Theta(\omega, \omega_0) = \frac{3}{8} \frac{\pi K(\omega_0)}{m_0c} \frac{\omega_0}{\omega_0^2 - \omega^2 + 4(\tau_1 + \tau_2)^2} \left[ (\tau_1 + \tau_2) \right. \\ \left. + 2 \sum_{j=m, 1} \frac{\tau_1 + \tau_2 + \tau_j}{(\omega_0 - \omega)^2 + \tau_j^2} \right]. \end{aligned} \quad (21)$$

When the frequencies are noticeably different, so that  $|\omega_0 - \omega| \gg \gamma_1$ , Eq. (21) becomes Eq. (12).

For  $\gamma_2 \gg \gamma_1$ , in the frequency range  $(\omega_0 - \omega)^2 \ll 4\gamma_1\gamma_2$ ,

$$\Theta(\omega, \omega_0) \approx \frac{\tau_2(\omega_0 - \omega)}{(\omega_0 - \omega)^2 + \tau_2^2}. \quad (22)$$

In this case, the main contribution to the nonlinear susceptibility which determines the optical rotation comes from a sequence of two processes: a hole transition from the state  $(1, \mathbf{k})$  to the state  $(2, \mathbf{k} + \mathbf{q}_0)$  with absorption of a photon  $\hbar\omega_0$  and one from the state  $(2, \mathbf{k} + \mathbf{q}_0)$  to the state  $(1, \mathbf{k} + \mathbf{q}_0 - \mathbf{q})$  with emission of a photon  $\hbar\omega$ . These two processes may also be regarded as a resonant scattering of light:  $(1, \mathbf{k}) + \hbar\omega_0 \rightarrow (1, \mathbf{k} + \mathbf{q}_0 - \mathbf{q}) \rightarrow \omega$ . This explains why the rotation angle (22) is proportional to the lifetime of the excited state  $(2, \mathbf{k} + \mathbf{q}_0)$ , whereas the dependence of the rotation angle on the difference  $(\omega_0 - \omega)$  is governed by the damping of the initial and final states, i.e., by  $2\gamma_1 + \tau_1^2$ . The frequency dependence (21) is more complex than the dependence (22). The reason is that, in addition to the resonant scattering of light, there is a contribution to the nonlinear susceptibility from the decrease in the population of the heavy hole states with  $\mathbf{k} \approx \mathbf{k}_0$ , which in particular reduces the absorption coefficient at the frequency  $\omega$ . The maximum value of  $\Theta(\omega, \omega_0)$  as a function of the frequency  $\omega$  for  $\gamma_2 \gg \gamma_1$  is

$$\Theta_{\text{max}} = \frac{3}{16} \frac{\pi K(\omega_0)}{m_0c^2 \omega_0^2} \frac{\tau_1^2 \tau_2}{\tau_1^2 + \tau_2^2}. \quad (23)$$

## 2. EXPERIMENTAL RESULTS AND DISCUSSION

1) Experiments to detect the effects described above used two light beams from a single Q-switched  $\text{CO}_2$  laser, pulse duration  $10^{-7}$  sec, repetition frequency  $5 \cdot 10^4$  sec<sup>-1</sup>, and wavelength  $\lambda = 10.6 \mu$ . One beam was strong and used for pumping, the other, a linearly polarized weak beam, was used for probing. Figure 1 shows a diagram of the experiment.

Samples of p-type InAs with hole density  $p = (8-9) \cdot 10^{15} \text{ cm}^{-3}$  were cut in a wedge shape with angle 3.5°. For measurement, they were placed on the heat sink of a nitrogen cryostat and fixed there by light blade springs. The sample temperature in the experiments was held at 90±2 K. The radiation in each beam transmitted through the sample was monitored by the detectors  $\text{PD}_1$ ,  $\text{PD}_2$ . The probe radiation then passed through an analyzer with polarization ratio 1:4·10<sup>4</sup> and either directly to the detector or, as in Fig. 1, first through an IKM-1 monochromator with a 100 lines/mm diffraction grating.

In the path of the strong beam was a quarter-wave or half-wave phase polarizer to change the pump radiation

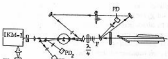


Fig. 1. Diagram of the experiment to detect photoinduced gyrotropy and anisotropy.

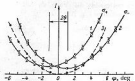


FIG. 2. Dependence of the probe radiation flux on the analyser rotation angle  $\phi$  for a p-type InAs crystal with  $p = 9 \cdot 10^{11} \text{ cm}^{-3}$  at  $90 \text{ K}$ : 1) right-hand circularly polarized pump radiation  $\omega_{\perp}$ ; 2) left-hand circularly polarized pump radiation  $\omega_{\perp}$ ; 3) linearly polarized pump radiation with  $e^{(1)} \parallel \omega$ .

polarization. By rotating the analyser through the angle  $\phi$ , the dependences  $I(\phi)$  with  $\omega \parallel e^{(1)}$  and with left-hand or right-hand circular polarization of the pump radiation were measured. In the study of the effect of linearly polarized pump radiation, we also measured  $I(\phi)$  for  $\psi = (\theta, \omega_{\perp}) = \pm \pi/4, \pm \pi/2$ .

Figure 2 shows the dependences of the probe radiation flux  $I$  on the angle  $\phi$  for circularly polarized pump radiation ( $\sigma_{\pm}$ ) and also, for comparison, the corresponding dependence for linearly polarized pump radiation with  $e^{(1)} \parallel \omega$ . It is seen that for  $\sigma_{\pm}$  polarization the polarization plane of linearly polarized probe radiation is rotated through  $\theta \approx 1^\circ$ . The angle of rotation per unit length, related to the observed angle  $\theta$  by  $\theta = \theta_{\text{K}}/(1 - e^{-Kd})$ , where  $d$  is the crystal thickness, is  $16^\circ/\text{cm}$ . There is also some upward shift of the  $I(\phi)$  curves. This is due to the slight ellipticity induced, which evidently results from the difference between the imaginary parts of  $\delta\omega_{\sigma_{\pm}}, \omega_{\perp}, \theta_{\sigma_{\pm}}, \omega_{\perp}$  in Eq. (18), which determines the photoinduced circular dichroism.

Similar dependences  $I(\phi)$  are found for linearly polarized pump radiation with  $\psi = \pm \pi/4$ , together with a rotation of the probe radiation polarization plane (because of the induced dichroism) and ellipticity of this radiation (because of the induced birefringence). The latter is a periodic function of  $\phi$  with period  $\pi/2$ .

2) The theoretical part of this paper gave a calculation of the polarization plane rotation angle due to hole orientation in direct transitions between valence subbands 1 and 2. However, other mechanisms may also contribute to the optical rotation. The induced gyrotropy effect due to nonlinear polarization of bound valence electrons by circularly polarized light has been calculated.<sup>3</sup> This effect has been observed<sup>10</sup> in n-type indium arsenide ( $p \approx 1.6 \cdot 10^{16} \text{ cm}^{-3}$ ) at  $T = 90 \text{ K}$ , but the rotation angle was due mainly not to valence electrons but to electrons in the conduction band, and was found<sup>11</sup> to increase considerably with the density of these electrons.

In this connection, it was necessary to make sure that the induced gyrotropy effect observed in p-type InAs is indeed due to absorption by holes. For that purpose, in particular, an experiment was performed in which, under identical conditions (at  $90 \text{ K}$  and equal pump radiation intensity), we measured the rotation angles for n-type and p-type samples having the densities mentioned above. It was found that the rotation angle in a p-type

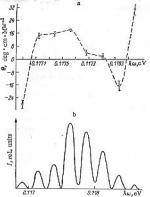


FIG. 3. Spectrum  $\Theta(\theta, \omega)$  of the probe radiation polarization plane rotation angle for circularly polarized pump radiation (a); spectrum of the strong and probe radiation transmitted through the sample (b).

sample is about eight times the value in an n-type sample. This indicates that we may neglect the contribution to the observed rotation angle in p-type InAs from the induced gyrotropy resulting from the nonlinear polarizability of bound electrons.

The induced rotation was measured for a p-type InAs sample at a higher temperature also,  $T \approx 160 \text{ K}$ . It is known that the absorption coefficient for  $10 \mu\text{m}$  radiation in p-type InAs and the hole mobility (and therefore the momentum relaxation times) decrease with rising temperature. It follows from Eq. (21) that the maximum rotation angle  $\Theta(\omega, \omega_0)$  should be proportional to the absorption coefficient and the product of the relaxation times  $\tau_1$  and  $\tau_2$ . As we should expect, the rotation angle  $\Theta$  at  $160 \text{ K}$  is less (by a factor of about 2) than at  $90 \text{ K}$ .

It has been shown in the theoretical section that the induced gyrotropy effect due to optical orientation of holes is a resonance one and should decrease with increasing  $|\omega - \omega_0|$  when  $|\omega - \omega_0| \gg \gamma_1, \gamma_2$ . To test this, we did experiments with pump radiation photon energy  $\hbar\omega_0 = 0.117 \text{ eV}$  and probe radiation photon energy  $\hbar\omega = 0.234 \text{ eV}$ . In this case, the rotation angle was an order of magnitude less than for probe radiation with  $\hbar\omega = 0.117 \text{ eV}$ . Approximately the same relation was found for linearly polarized pump radiation and the induced ellipticity with probe radiation in these spectrum lines, which confirms the resonance nature of the observed effect and its association with direct hole transitions between subbands of the valence band.

The theoretical prediction of a sharp resonance of these effects in the range  $\omega \approx \omega_0$  made it necessary to verify the presence of rotation angle dispersion near the resonance. Note that in all the experiments we used laser radiation whose spectrum consisted of eight close and equidistant narrow lines (Fig. 3), the total width of the spectrum not exceeding  $1.7 \text{ meV}$ . It was thus possible to measure the rotation angle for each line of the probe

beam (the crystal being pumped with spectrally unresolved circularly polarized radiation). For this purpose, the probe radiation, after passing through the sample, was put through a monochromator, and the energy dependence of the polarization plane rotation angle was measured. Figure 3 shows the spectrum  $\Theta(\Omega)$  thus found; note that the angular dependences in Fig. 2 were obtained for the probe radiation line  $\hbar\omega = 0.11762$  eV. It is seen from this spectrum that there is strong dispersion of the rotation angle  $\Theta(\Omega)$ . In particular, the value of  $\Theta$  has in this energy range (1.7 meV) three changes of sign. The presence of a strong dispersion  $\Theta(\Omega)$  confirms that the induced gyrotropy in p-type InAs is a resonance effect. However, the form of the spectrum cannot be described in terms of the theory given above, since that was based on the assumption that each beam is monochromatic and that spectrally unresolved radiation was incident on the crystal in the experiment.

Since the  $\text{CO}_2$  laser radiation spectrum is a set of equidistant narrow lines, an effective rotation at the frequency  $\omega$  of some harmonic of the probe field can also result from a nonlinear interaction of the type  $\hbar\omega = \hbar\omega_0 - \hbar\omega_2 + \hbar\omega'$ , where  $\omega_0$  and  $\omega_2$  are the frequencies of two harmonics of the strong light wave, and  $\omega'$  that of a harmonic of the probe wave. The effective specific rotation angle at frequency  $\omega$  due to the nonlinear process in question is given by

$$\Theta = \frac{3}{8} \text{e}K(\omega) (I_{01}I_{02}I')^{1/2} \frac{e^2}{c\omega_0\omega_2} \text{Re} \left\{ \frac{\exp[i(\varphi_{01} - \varphi_{02} + \varphi' - \varphi)]}{\omega_0 - \omega_2 - \omega' - 2\varphi} \frac{1}{(\varphi_0 + \varphi_2)} \right. \\ \left. \times \sum_{j=1,2} \left( \frac{1}{i(\omega_0 - \omega_2) + 2\varphi_j} + \frac{1}{i(\omega_0 - \omega') + 2\varphi_j} \right) \right\}, \quad (24)$$

where  $I_{01}$ ,  $I_{02}$ ,  $I'$ , and  $I$  are the harmonic intensities at  $\omega_0$ ,  $\omega_2$ ,  $\omega'$ , and  $\omega$ ;  $\varphi_{01}$ ,  $\varphi_{02}$ ,  $\varphi'$ , and  $\varphi$  their phases at the nonlinear interaction point. It is clear that the rotation angle values resulting from the combined nonlinear interaction of the light waves must be similar in order of magnitude to the angle for two monochromatic beams with  $|\omega - \omega_0 - \omega_2 - \omega'|$ . Since the phase differences of the various laser radiation lines are unknown,<sup>13</sup> it is not yet possible to construct a theoretical spectrum in accordance with the experimental conditions. However, the experimental re-

sults as a whole show that it is reasonable to suppose that the form of the  $\Theta(\Omega)$  spectrum in Fig. 3 is substantially the result of four-wave nonlinear interaction between the probe and strong beams.

Comparison of the observed values of the maximum rotation angle with Eq. (21) gives a lower limit to the product of the relaxation times:  $\tau_1\tau_2 > 6 \cdot 10^{-25}$  sec<sup>2</sup>. This is reasonable, since the mean heavy hole relaxation time which determines the hole mobility is  $\langle\tau_1\rangle = 1.6 \cdot 10^{-11}$  sec.

In order to make a detailed comparison of the experimental results with our theory, and determine the characteristic times  $\tau_1$  and  $\tau_2$ , we intend to carry out similar experiments with two monochromatic beams.

<sup>13</sup>However, the true width of the harmonic lines is unknown. The line widths in Fig. 2 are apparently of instrumental origin.

<sup>1</sup> Yu. P. Zakharchenko, in: *Problems of Modern Physics in Russia*, Nauka, Leningrad, 1970, p. 180.  
<sup>2</sup> Yu. P. Zakharchenko, D. N. Mirlin, V. L. Perel', and I. I. Rodina, *Usp. Fiz. Nauk* **136**, 459 (1982) [Sov. Phys. Usp. **25**, 143 (1982)].  
<sup>3</sup> A. G. Aronov and E. I. Fedorova, *Fiz. Tverd. Tela* (Leningrad) **15**, 231 (1973) [Sov. Phys. Solid State **15**, 160 (1973)].  
<sup>4</sup> A. M. Danilevskii, S. P. Kochergin, and V. K. Sushkov, Abstracts of Papers presented at All-Union Conf. on Semiconductor Physics in Russia, Elm, Ural, 1982, p. 155.  
<sup>5</sup> G. L. Hu and G. E. Pake, *Symmetry and Strain-Induced Effects in Semiconductors*, Israel Program for Scientific Translations, Jerusalem; Wiley, New York, 1975.  
<sup>6</sup> S. G. Epstein, G. T. Stumbo, and A. M. Shluger, *Nonlinear Resonances in Atomic and Molecular Spectra* [in Russian], Naukova, Novosibirsk, 1975.  
<sup>7</sup> F. Kellman, IEEE J. Quantum Electron., **QE-15**, 629 (1979).  
<sup>8</sup> R. B. James and D. L. Smith, *Phys. Rev. Lett.* **35**, 1495 (1975).  
<sup>9</sup> E. Yu. Perlin, *Fiz. Tverd. Tela* (Leningrad) **23**, 66 (1981) [Sov. Phys. Solid State **23**, 38 (1981)].  
<sup>10</sup> A. M. Danilevskii, S. P. Kochergin, and V. K. Sushkov, *Radiotekhnika i elektronika*, **33**, 656 (1988) [Sov. Phys. Usp. **33**, 611 (1988)].  
<sup>11</sup> A. M. Danilevskii, S. P. Kochergin, and V. K. Sushkov, Abstracts of Papers presented at Eleventh All-Union Conf. on Coherent and Nonlinear Optics, Erevan, 1982 [in Russian], p. 396.

Translated by J. B. Sykes